DOI 10.1007/s10946-021-10010-5
Journal of Russian Laser Research, Volume 42, Number 6, November, 2021

TWO-PHOTON EXCITED LUMINESCENCE OF NV-CENTERS AND STIMULATED RAMAN SCATTERING IN NANODIAMONDS†

A. D. Kudryavtseva,[1*] M. A. Shevchenko,[1] N. V. Tcherniega,[1] S. F. Umanskaya,[1] and A. N. Baranov[2]

[1] *Lebedev Physical Institute, Russian Academy of Sciences Leninskii Prospect 53, Moscow 119991, Russia*

[2] *Faculty of Physics, Lomonosov Moscow State University Vorob'evy Gory 1/2, Moscow 119991, Russia*

*Corresponding author e-mail: akudr@sci.lebedev.ru

Abstract

In this study, zero-phonon line (ZPL) at 638 nm associated with multiphoton excited negatively-charged single nitrogen-vacancy (NV)-center luminescence is registered in ethanol suspension of submicrometer diamond particles obtained at high pressures and high temperatures (HPHT). Simultaneously Stokes and anti-Stokes components of the stimulated Raman scattering (SRS) in the same sample is registered with a frequency shift of 1332 cm^{-1} corresponding to the fundamental optical mode of the diamond crystal. We observe anti-Stokes component intensity enhancement caused by its wavelength coincidence with the wavelength of luminescence caused by negatively-charged single nitrogen-vacancy (NV) centers.

Keywords: zero phonon line, Raman scattering, anti-Stokes luminescence, wavelength.

1. Introduction

Luminescence in the region with wavelengths shorter than excitation wavelength is called anti-Stokes luminescence or up-conversion. Now it is being wudely studied not only because of important fundamental aspects but also because of numerical practical applications [1]. It can be used in solar energy conversion [2], in microbiology for super-resolution bioimaging [3], for drug delivery with high degree of control over drug delivery processes [4], for fluorescent bioprobes creation [5], and for damage detection and monitoring of civil, aerospace, and military structures [6]. The processes, leading to anti-Stokes luminescence, may be different. In complex organic compounds, it can be triplet–triplet annihilation-based photon up-conversion (TTA-UC), which implicates a sequence of photo-physical processes in dyes [7, 8]. In solids (some crystals or nanostructures like synthetic opals), processes near to triboluminescence can lead to bright light emission in the blue–green range [9, 10]. Under cooling, such emission can have duration up to few seconds under nanosecond or picosecond laser excitation [11–13].

One of important processes leading to the anti-Stokes luminescence is multiphoton excitation. Two-photon excited luminescence was registered in different materials – organic liquids [14], crystals [15],

†We dedicate this paper to Professor Vladimir S. Gorelik, our friend and collaborator during many years; this study is a continuation of our fruitful collaboration.

Manuscript submitted by the authors in English on August 9, 2021.

nanostructures [16], polymers [17], and in pharmaceutical and biologically active solid-state materials [18]. Anti-Stokes luminescence can be a result of crystalline lattice defects. For instance, we observed long-lasting anti-Stokes luminescence in frozen suspension of ZnS nanoparticles [19]. Under nanosecond laser-pulse excitation at a wavelength of 694.3 nm, we observed emission band in the range from 489 to 510 nm, which had duration up to 3 s. The luminescence band centered at about 480 nm is usually attributed to the Zn^{2+}-vacancy levels [20]. The green band at 510 nm is associated with sulfur species on the surface of the ZnS nanoparticles [21].

One of the kinds of crystal lattice defects is nitrogen-vacancy-center (NV-center) formation in diamond, when a carbon atom in a crystal lattice site is replaced by a nitrogen atom. The centers can exist in negative (NV^-) [22, 23] and neutral (NV^0) [24] charge states. The identifying features of NV^- and NV^0 are their optical zero-phonon lines (ZPLs) at 637 nm [24] and at 575 nm, respectively, and associated vibronic bands that extend from their ZPLs to lower energy in the luminescence spectrum [25, 26]. The NV-center's electron spin can be manipulated by external factors, such as different electromagnetic fields resulting in sharp resonances in the photoluminescence intensity. These resonances can be explained in terms of electron-spin related phenomena and analyzed using advanced quantum theory. An individual NV center can be used as a basic unit for a quantum computer. The diamond luminescence caused by negatively-charge single nitrogen-vacancy (NV^-) centers was registered in 1997 [27] and became an important point in the development of diamond-based quantum technologies. We found out that ZPL coincides with first anti-Stokes Raman line in diamond.

Diamond is a very important material for science and technology because of its unique properties – the largest thermal conductivity of any known substances and low thermal expansion coefficient. Due to its optical properties (high Raman gain coefficient, large Raman shift, transparency between $\lambda = 230$ nm and $\lambda = 2500$ nm) diamond is used in optics, mainly as Raman convertor. Raman scattering was first observed in natural diamond in 1930 [28]. In accordance with theory, the fundamental F_{2g} symmetry mode is registered in Raman scattering in diamond with a frequency shift of 1332 cm^{-1} corresponding to the vibrations of two interpenetrating cubic diamond sublattices.

For the first time, the stimulated Raman scattering (SRS) in natural diamond was registered in [29] and then studied in [30]. Wide practical applications of diamond became possible when different methods of synthesis of nanodiamonds (NDs) were developed. NDs were first produced by detonation in 1963. Later, especially in 1990's, great progress was achieved in ND synthesis, purification, and isolation techniques. Today NDs can be synthesized in large quantities at a relatively low cost. Synthesis techniques include detonation, laser ablation, high-pressure high-temperature (HPHT) technique, plasma-assisted chemical vapor deposition (CVD), autoclave synthesis from supercritical fluids, chlorination of carbides, ion irradiation of graphite, and ultrasound cavitation. In this work, we use HPHT NDs with radius of 250 nm.

2. Samples and Experimental Setup

In the experiments, as a sample, we use ethanol suspension of monodisperse nanodiamonds obtained with the help of high-pressure high-temperature (HPHT) method. We measured dimensions of nanodiamonds, in view of dynamic light scattering; the result is shown in Fig. 1. NDs radius was found to be 250 nm.

The NDs suspension concentration was about 10^{11} cm^{-3}. Suspension was put into the quartz cell with a length of 1 cm. We show the transmittance of the cell with suspension in Fig. 2 and the experimental

setup for SRS and luminescence investigations, in Fig. 3.

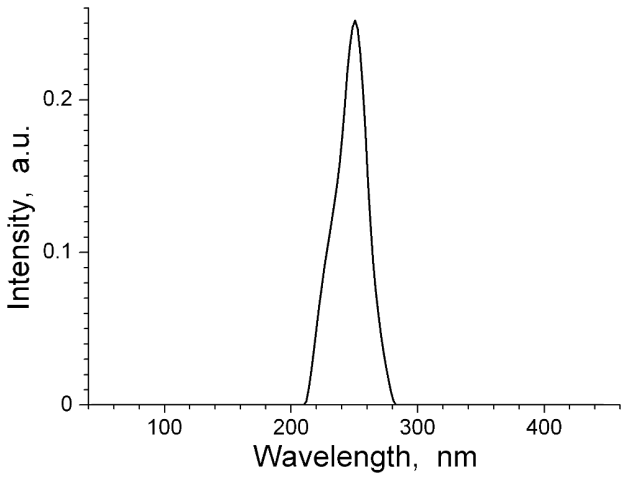

Fig. 1. Distribution of hydrodynamic radius of diamond nanoparticles in ethanol.

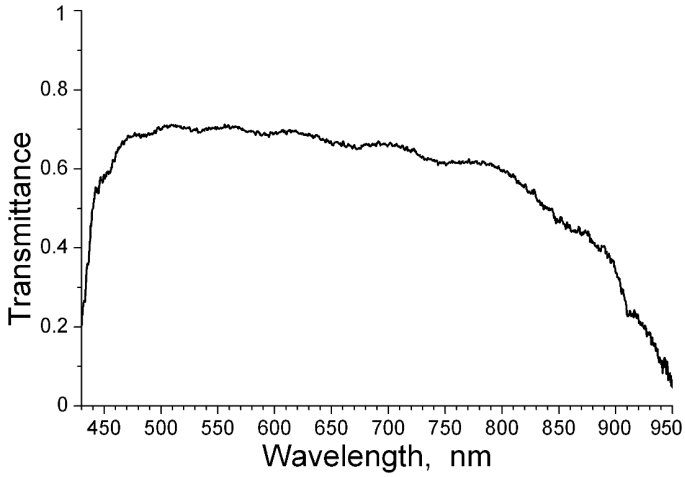

Fig. 2. The transmittance of the cell with nanodiamond ethanol suspension.

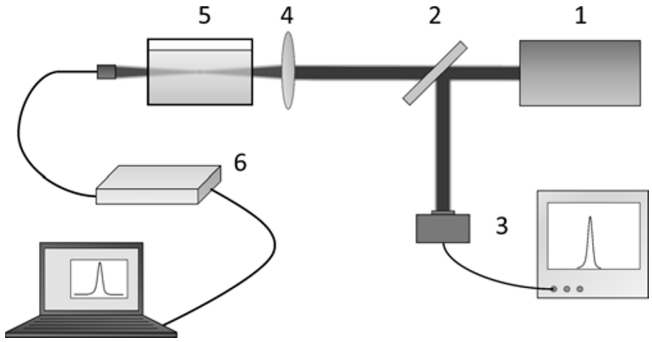

Fig. 3. Experimental setup for SRS study with a ruby laser 1, glass plate 2, the system for laser pulse characteristics measurements 3, lens 4, a quartz cell with the sample 5, and a minispectrometer connected to PC 6.

For excitation, we used nanosecond pulses of Q-switched ruby laser ($\lambda = 694.3$ nm, $E_{\max} = 0.6$ J, $\tau_p \approx 20$ ns, $\Delta\nu = 0.015$ cm^{-1}, divergence $3.5 \cdot 10^{-4}$ rad). The laser light was focused by a 5 cm lens on the sample. The energy of the laser pulse could be varied. It provided the possibility to define the energetic characteristics of the scattered light.

3. Experimental Results

For the sample under investigation, an increase in the laser energy led to effective SRS excitation with a threshold of ~0.75 GW/cm^2. SRS spectrum contained the 1$^{\text{st}}$ Stokes component with a wavelength of 765 nm and the 1$^{\text{st}}$ anti-Stokes component with a wavelength of 635.5 nm. The anti-Stokes component of SRS spectrum in ethanol suspension of diamond particles is shown in Fig. 4. The maximum conversion efficiency of the exciting light into SRS was 7%. The experimental threshold I_{th} under given experimental conditions was estimated to be 0.75 GW/cm^2. Raman gain was estimated to be 40 cm/GW. Point out

that, at the laser intensity used, no SRS signal corresponding to ethanol was registered. The evolution of the anti-Stokes part of the scattered radiation spectrum is shown in Fig. 4.

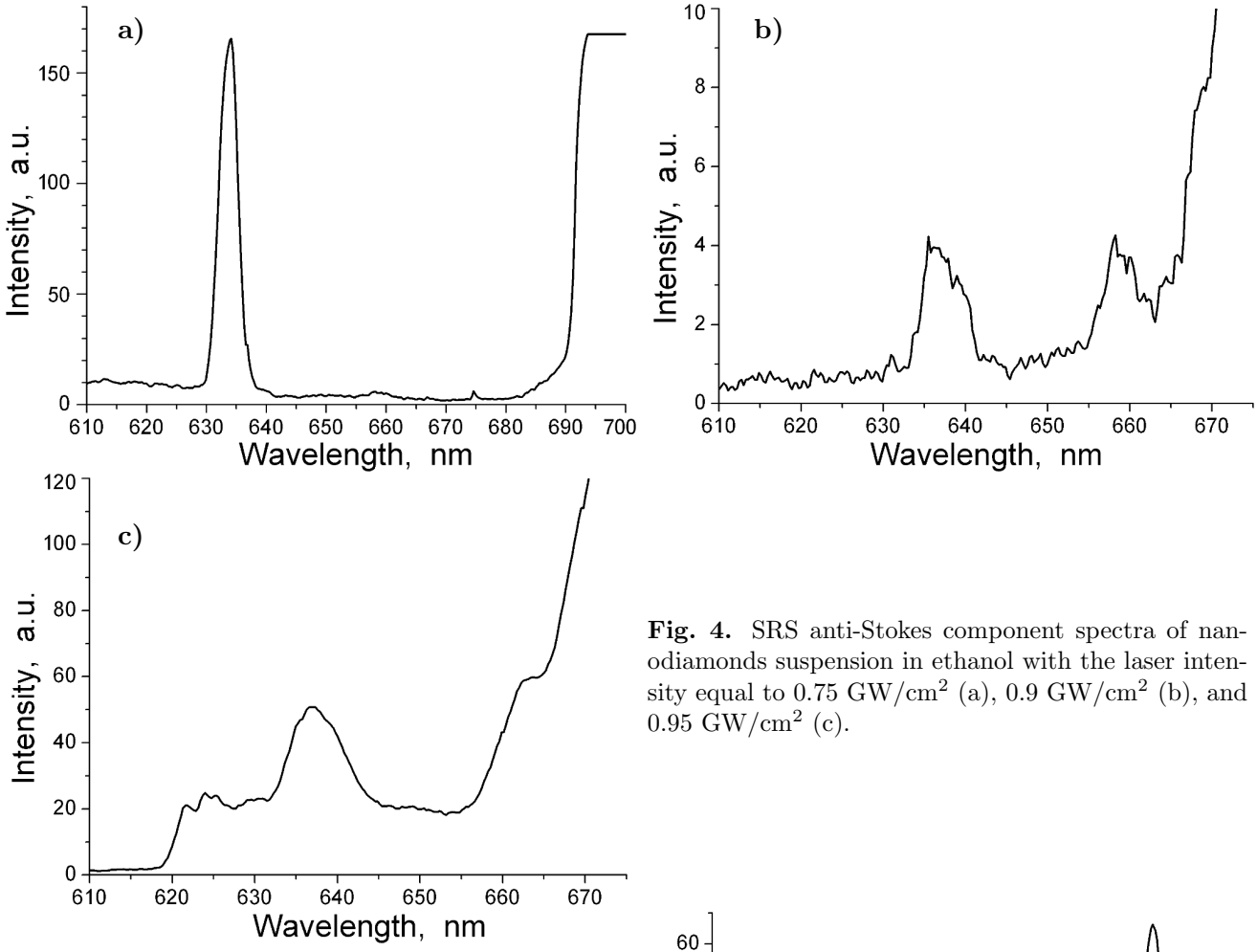

Fig. 4. SRS anti-Stokes component spectra of nanodiamonds suspension in ethanol with the laser intensity equal to 0.75 GW/cm^2 (a), 0.9 GW/cm^2 (b), and 0.95 GW/cm^2 (c).

At the laser intensity corresponding to the SRS threshold value (Fig. 4 a), only one spectral component corresponding to the first anti-Stokes component is excited. Increase in the laser intensity leads to excitation of the luminescence caused by negatively-charged single nitrogen-vacancy (NV) centers and accordingly to a significant broadening of the spectrum (Fig. 4 c, d).

To obtain the luminescence caused by negatively-charged single nitrogen-vacancy (NV)-centers, it was necessary to increase laser intensity reaching more than 0.9 GW/cm^2. Under these conditions, we registered more detailed spectrum of our sample emission in the region of SRS anti-Stokes com-

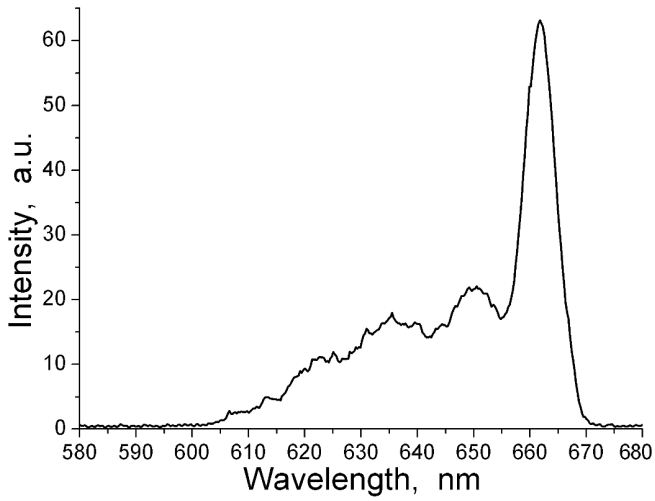

Fig. 5. Spectrum of ZPL and anti-Stokes SRS component in NDs ethanol suspension.

ponent. The spectrum corresponding to the laser intensity equal to 1 GW/cm^2 is presented in Fig. 5. A notch filter was used to suppress strait laser light.

The band at 638 nm corresponds to ZPL, and lines at lower frequencies are accompanying it vibronic bands. As one can see in Fig. 5, wavelengths of ZPL and SRS anti-Stokes component in ethanol NDs suspension are very close; this fact provides the five-hold anti-Stokes component intensity increase.

4. Summary

We showed that the anti-Stokes radiation intensity could be enhanced essentially in the presence of the luminescence caused by negatively-charged single nitrogen-vacancy (NV^-)-centers simultaneously with the SRS anti-Stokes component. This situation can be only realized in the case where the anti-Stokes SRS component frequency coincides with the luminescence frequency, and such a situation takes place only when a ruby laser is employed as the excitation source.

Acknowledgments

The authors acknowledge the financial support provided by the Russian Foundation for Basic Research under Projects Nos. 19-02-00750_a, 19-02-00440_a, and 20-52-00002-Bel_a, as well as the Belarus Foundation for Basic Research under Grant F20R-013.

References

1. N. Murase, R. Jagannathan, Y. Kanematsu, et al., *J. Phys. Chem. B*, **103**, 754 (1999).
2. Y. Shang, S. Hao, C. Yang, and G. Chen, *Nanomaterials*, **5**, 1782 (2015).
3. S. Xu, S. Huang, Q. He, and L. Wang, *Trends Analyt. Chem.*, **66**, 72 (2015).
4. Yue Guan, Hongguang Lu, Wei Li, et al., *ACS Applied Materials & Interfaces*, **9**, 26731 (2017).
5. U. Bazylinska, J. Kulbacka, D. Wawrzynczyk, and R. Frackowiak, *Sci. Rep.*, **6**, 29746 (2016).
6. D. O. Olawale, T. Dickens, W. G. Sullivan, et al., *J. Lumin.*, **131**, 1407 (2011).
7. C. A. Parker and C. G. Hatchard, *Proc. R. Soc. London, Ser. A*, **269**, 574 (1962).
8. Y. C. Simon and C. Weder, *J. Mater. Chem.*, **22**, 20817 (2012).
9. Y. Kawaguchi, *Phys. Rev. B*, **52**, 9224 (1995).
10. N. V. Tcherniega, A. D. Kudryavtseva, and M.I. Samoylovich, *J. Surface Investigation: X-ray, Synchrotron and Neutron Techniques*, **2**, 624 (2008).
11. N.V. Tcherniega and A.D. Kudryavtseva, *J. Surface Investigation: X-ray, Synchrotron and Neutron Techniques*, **3**, 513 (2009).
12. N. A. Bulychev, M. A. Kazaryan, A. D. Kudryavtseva, et al., *Proc. SPIE*, **10614**, 106140N (2018).
13. A. Anjiki and T. Uchino, *J. Phys. Chem. C*, **116**, 15747 (2912).
14. V. S. Gorelik, A. D. Kudryavtseva, A. I. Sokolovskaya, and N. V. Tcherniega, *Opt. Spectrosc.*, **18**, 369 (1996).
15. V. S. Gorelik, A. M. Agaltzov, L. I. Zlobina, *J. Mol. Structure*, **266**, 121 (1992).
16. M. V. Vasnetsov, V. Yu. Bazhenov, I. N. Dmitruk, et al, J. *Luminescence*, **166**, 233 (2015).
17. M. Tareeva, M. Shevchenko, S. Umanskaya, et al., *J. Russ. Laser Res.*, **41**, 502 (2020).
18. V. S. Gorelik and E. A. Kozulin, *Quantum Electron.*, **24**, 462 (1994).
19. H. Ehrlich, A. Kudryavtseva, G. Lisichkin, et al., *Int. J. Thermophys.*, **36**, 2784 (2015).
20. N. Murase, R. Jagannathan, Y. Kanematsu, et al., *J. Phys. Chem. B*, **103**, 754 (1999).
21. Changhui Ye, Xiaosheng Fang, Guanghai Li, and Lide Zhang, *Appl. Phys. Lett.*, **85**, 3035 (2004).
22. J. H. N. Loubser and J. A. van Wyk, *Diamond Res.*, **77**, 11 (1977).

23. J. H. N. Loubser and J. A. van Wyk, *Rep. Prog. Phys.*, **41**, 1202 (1978).
24. Y. Mita, *Phys. Rev. B*, **53**, 11360 (1996).
25. Yu. D. Glinka, K.-W. Lin, and S. H. Lin, *Appl. Phys. Lett.*, **74**, 236 (1999).
26. V. Zhicheng, *J. Mater. Chem. C*, **7**, 8086 (2019).
27. A. Gruber, A. Drabenstedt, C. Tietz, et al., *Sci.*, **276**, 2012 (1997)
28. R. Robertson and J. J. Fox, *Nature (London)*, **125**, 704 (1930).
29. P. G. Eckhard, D. P. Bortfeld, and M. Geller, *Appl. Phys. Lett.*, **3**, 137 (1963).
30. A. K. McQuillan and B. P. Stoicheff, *Bulletin Am. Phys. Soc.*, **12**, 60 (1967).